# Improvement of Shielding Models with *h*-Conformal Formulation using a Subproblem Finite Element Technique

Vuong Dang Quoc

***Abstract***— *The aim of this work is to present an extension of the subproblem finite element approach to improve inaccuracies around curvatures and corners from thin shell finite element models. Traditional shielding magnetic models are generally replaced by surfaces with impedance-type interface conditions, which accept inaccuracies of the local solutions surrounding corners and borders such as magnetic fields, eddy current losses and Joule power losses. In this article, the extended subproblem approach is performed with the h-conformal finite element formulation where the shielding models are coupled in a sequence of a three step-coupling: Stranded inductors alone (step 1) – added shielding models (step 2)- volume corrections (step 3). Each step of the method allows separately solving on its own sub-domain and meshing without starting again a full problem for each new set of parameters. This leads to a reduced computational time.*

***Keywords***— **Eddy current, joule power loss, magnetodynamics, subproblem technique, thin shell approximations.**

## 1. INTRODUCTION

The direct use of the finite element method (FEM) formulation to realistic thin plates in electromagnetic shielding problems is still extremely challenging, even not possible [1]. For magnetodynamic problems, when thin shells are conducting, very thin meshes have to be created to capture the skin depth, this becomes more and more computationally expensive (and difficult) with increasing frequency.

So as to scope with this advantage, in [2], [3], the classical thin shell (TS) solution is proposed to replace volume thin meshes (Fig. 1, *left*) by surface meshes with impedance-type interface conditions (ICs) (Fig. 1, *right*), but this approximation neglects significant errors in the calculation of local quantities (magnetic flux density, magnetic field, eddy current and joule power loss…) around corners and edges.

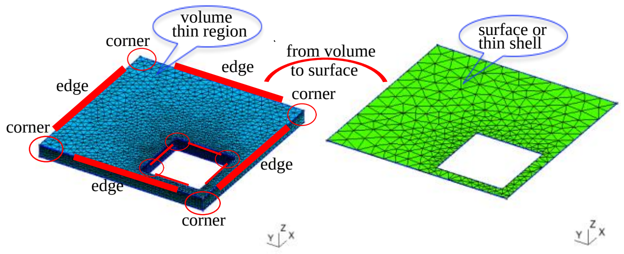


**Fig. 1: From volume (*left*) to surface (*right*).**

In order to overcome this drawback, many studies have recently developed a subproblem method (SPM) for one-way coupling to improve inaccuracies near corners and edges occurring from the TS [4]-[7], or to correct errors in conducting regions and global fields [8]-[10].

Dang Quoc Vuong is Director of Training Center of Electrical Engineering, School of Electrical Engineering, Hanoi, University of Science and Technology. Email: vuong.dangquoc@hust.edu.vn

In this paper, a three step-coupling technique with the ***h***-conformal magnetodynamic finite element (FE) formulation is extended from a one-way coupling to treat inaccuracies on local electromagnetic solutions from the TS approximations [2], [3]. The extended method is implemented as a sequence, allowing to divide a full problem (including of stranded inductors and magnetic thin regions) into three steps:

- Step 1: A problem involving stranded inductors is first considered on a simplified mesh.
- Step 2: A thin shell is added with very coarse mesh that does not contain stranded inductor anymore.
- Step 3: A volume correction with an actual thin plate is improved errors of the TS solutions.

In this strategy SP, from the stranded inductor to the TS model is constrained by surface sources (SSs) that indicate changes of ICs across surfaces [4]-[6]. From the TS model to the volume correction is constrained by SSs and volume sources (VSs), where VSs present changes of material properties (i.e., permeability and conductivity) of volume thin regions [4]-[6].

Each process of the method allows separately doing on its own domain and meshing without depending on the meshes and domains of other subproblems (SPs). This also permits to consider previous solutions as SSs or VSs for new SPs instead of solving a new full problem for each new set of parameters.

## 2. SEQUENCE OF SUBPROBLEM APPROACH

### *Magnetodynamic problem*

In the scenario of the subproblem approach, a magnetodynamic problem $q$ is performed at step $q$ in a domain $\Omega_q$, with $\Omega_c = \Omega_{c,q} \cup \Omega_{c,q}^C$ and the boundary $\partial\Omega_q = \Gamma_q = \Gamma_{h,q} \cup \Gamma_{b,q}$. Where $\Omega_{c,q}$ and $\Omega_{c,q}^C$ are respectively the conducting part and the non-conducting. The Maxwell's equations together with the following constitutive relations express [4] - [8].

$$\text{curl}\,\boldsymbol{h}_q = \boldsymbol{j}_{s,q}, \text{div}\boldsymbol{b}_q = 0, \text{curl}\boldsymbol{e}_q = -\partial_t \boldsymbol{b}_q, \quad \text{(1a-b-c)}$$

$$\boldsymbol{b}_q = \mu_q \boldsymbol{h}_q + \boldsymbol{b}_{s,q},\ \boldsymbol{e}_q = \sigma_q^{-1}\boldsymbol{j}_q + \boldsymbol{e}_{s,q}, \quad \text{(2a-b)}$$

$$\boldsymbol{n}\times \boldsymbol{e}_q|_{\Gamma_{e,q}} = 0, \quad [\boldsymbol{n}\times\boldsymbol{e}_q]_{\gamma_q} = \boldsymbol{k}_{f,q}, \quad \text{(3a-b)}$$

where the source fields ($\boldsymbol{b}_{s,q}$ and $\boldsymbol{e}_{s,q}$) in (2 a-b) are VSs and $\boldsymbol{n}$ is the unit normal exterior to $\Omega_q$. The trace of electric field in (3 a) is defined as a zero for classical homogeneous boundary conditions (BCs). The discontinuity of electric field in (3 b) ($\boldsymbol{k}_{f,q}$) is a SS expressed its discontinuity through the positive and negative sides ($\gamma_q^+$ and $\gamma_q^-$) of any interface $\gamma_q$ in $\Omega_q$, with notation $[\cdot]_{\gamma_p} = |_{\gamma_p^+} - |_{\gamma_p^-}$ [4]-[7].

***Sequence of SPs: From stranded inductor alone to TS model***

As developed in [4]-[7], the constraint from stranded inductor alone to the TS models is expressed a SS (i.e. $\boldsymbol{k}_{f,q}$) in (3 b). This SS linked to the BC and IC is presented by the TS model associated with contributions from the previous problem [2], [3]. For the magnetic field formulation, the magnetic field is split as $\boldsymbol{h}_q = \boldsymbol{h}_{c,q} + \boldsymbol{h}_{d,q}$, where the fields $\boldsymbol{h}_{c,q}$ and $\boldsymbol{h}_{d,q}$ are respectively continuous and discontinuous components of $\boldsymbol{h}_q$ across the TS [3].

At the step 1, there is no any thin region in the stranded inductor, but it should be assumed that there is a relative constraint with the TS model across the ICs of the TS ($q = p$), with $\gamma_q = \gamma_q^\pm = \gamma_p^\pm$. For that, the trace discontinuity $[\boldsymbol{n}\times\boldsymbol{e}_p]_{\gamma_p}$ in (3 b) of the TS problem $p$ is given as [3]

$$[\boldsymbol{n}\times\boldsymbol{e}_p]_{\gamma_p} = [\boldsymbol{n}\times(\boldsymbol{e}_q+\boldsymbol{e}_p)]_{\gamma_p} = [\boldsymbol{n}\times\boldsymbol{e}]_{\gamma_p} = \mu_p\beta_p\partial_t(2\boldsymbol{h}_{c,p}+\boldsymbol{h}_{d,p}), \quad (4)$$

$$\boldsymbol{n}\times\boldsymbol{e}_p|_{\gamma_q^+} = \boldsymbol{n}\times(\boldsymbol{e}_q+\boldsymbol{e}_p)|_{\gamma_p^+} - \boldsymbol{n}\times\boldsymbol{e}_q|_{\gamma_p^+} = \frac{1}{2}\left[\mu_p\beta_p\partial_t(2\boldsymbol{h}_{c,p}+\boldsymbol{h}_{d,p}) + \frac{1}{\sigma_p\beta_p}\boldsymbol{h}_{d,p}\right] - \boldsymbol{n}\times\boldsymbol{e}_q|_{\gamma_p^+} = \frac{1}{2}\left[\mu_p\beta_p\partial_t(2\boldsymbol{h}_{c,p}+\boldsymbol{h}_{d,p}) + \frac{1}{\sigma_p\beta_p}\boldsymbol{h}_{d,p}\right] - \boldsymbol{k}_{f,q}, \quad (5)$$

where $\beta_p$ is given is [4]. In the stranded inductor (e.g. SP $q$), the trace discontinuity $[\boldsymbol{n}\times\boldsymbol{e}_p]_{\gamma_p}$ in (4) is equal to zero (i.e. $[\boldsymbol{n}\times\boldsymbol{e}]_{\gamma_p} = [\boldsymbol{n}\times\boldsymbol{e}_q]_{\gamma_q} + [\boldsymbol{n}\times\boldsymbol{e}_q]_{\gamma_p} = 0$) because it does not contribute to the solution of SP $q$ [3].

***Sequence of SPs: From TS model to volume correction***

The TS solution of the problem SP $p$ is next improved by the volume correction SP $k$ $(q = k)$ that scopes with the TS approximations [3]. So as to improve the TS model, one must remove the TS representation solution appearing in the SP $k$ by imposing a SS opposed to the TS IC. The changes of properties from the TS model to the volume correction are defined via the VSs ($\boldsymbol{b}_{s,k}$ and $\boldsymbol{e}_{s,k}$) in (2 a-b), i.e. [6], [9]

$$\boldsymbol{b}_{s,k} = (\mu_k - \mu_p)(\boldsymbol{h}_q + \boldsymbol{h}_p), \quad (6)$$

$$\boldsymbol{e}_{s,k} = -(\boldsymbol{e}_q + \boldsymbol{e}_p), \quad (7)$$

where the electric fields $\boldsymbol{e}_q$ and $\boldsymbol{e}_p$ are unknown and are defined via an electric problem [9].

## 3. SEQUENCE OF WEAK FORMULATIONS

From the results of Section 2, the weak formulations for each step coresponding to each SP are developed as the sequence: SP $q \rightarrow$ SP $p\rightarrow$ SP $k$.

***Step 1: A weak form for inductors – SP q***

The magnetic field formulation is written from the weak form of Faraday's equation (1 c) [5]-[10]. The field $\boldsymbol{h}_q$ is divided into two parts [6], [9], $\boldsymbol{h}_q = \boldsymbol{h}_{r,q} + \boldsymbol{h}_{s,q}$, where $\boldsymbol{h}_{r,q}$ is a reaction field and is unknown in advance, and $\boldsymbol{h}_{s,q}$ is a source field defined by a fixed current density such that $\text{curl}\,\boldsymbol{h}_{s,q} = \boldsymbol{j}_{s,q}$ in the stranded inductor $\Omega_{s,q}$. For the SP $q$, one gets

$$\partial_t(\mu_q\boldsymbol{h}_{r,q}, \boldsymbol{h}'_q)_{\Omega_q} + \partial_t(\mu_q\boldsymbol{h}_{s,q}, \boldsymbol{h}'_q)_{\Omega_q} + \langle\boldsymbol{n}\times\boldsymbol{e}_q, \boldsymbol{h}'_q\rangle_{\Gamma_{e,q}-\gamma_q} + \langle[\boldsymbol{n}\times\boldsymbol{e}_q]_{\gamma_q}, \boldsymbol{h}'_q\rangle_{\Gamma_q} = 0, \quad \forall\, \boldsymbol{h}'_q \in \boldsymbol{H}^1_{h,q}(\text{curl}, \Omega_q), \quad (8)$$

where the field $\boldsymbol{h}_{s,q}$ is determined via a projection method of the unknown distribution $\boldsymbol{j}_{s,q}$ [5], [6]. $H^1_{h,q}(\text{curl}, \Omega_q)$ is a function space including the basis function ($\boldsymbol{h}_{r,q}$) and the test function ($\boldsymbol{h}'_q$) as well. The term $\langle\boldsymbol{n}\times\boldsymbol{e}_q, \boldsymbol{h}'_q\rangle_{\Gamma_{e,q}-\gamma_q}$ is considered as a natural BC given in (3 a).

***Step 2: A weak form for TS model – SP p***

The weak form for the TS model SP $p$ is expressed via the terms $[\boldsymbol{n}\times\boldsymbol{e}_p]_{\gamma_p}$ and $\boldsymbol{n}\times\boldsymbol{e}_p|_{\gamma_q^+}$ given in (4) and (5), i.e.

$$\partial_t(\mu_p\boldsymbol{h}_p, \boldsymbol{h}'_p)_{\Omega_p} + (\sigma_p^{-1}\text{curl}\,\boldsymbol{h}_p, \text{curl}\,\boldsymbol{h}'_p)_{\Omega_{c,p}} + \langle\boldsymbol{n}\times\boldsymbol{e}_p, \boldsymbol{h}'_p\rangle_{\Gamma_{e,p}-\gamma_p} + \langle[\boldsymbol{n}\times\boldsymbol{e}_p]_{\gamma_p}, \boldsymbol{h}'_p\rangle_{\Gamma_p} = 0, \quad \forall\, \boldsymbol{h}'_p \in \boldsymbol{H}^1_{h,p}(\text{curl}, \Omega_p). \quad (9)$$

The test funcition $\boldsymbol{h}'_p$ in the trace discontinuity $\langle[\boldsymbol{n}\times\boldsymbol{e}_p]_{\gamma_p}, \boldsymbol{h}'_p\rangle_{\Gamma_p}$ in (10) is analysed as

$$\langle[\boldsymbol{n}\times\boldsymbol{e}_p]_{\gamma_p}, \boldsymbol{h}'_p\rangle_{\Gamma_p} = \langle[\boldsymbol{n}\times\boldsymbol{e}_p]_{\gamma_p}, \boldsymbol{h}'_{c,p} + \boldsymbol{h}'_{d,p}\rangle_{\Gamma_p} = \langle[\boldsymbol{n}\times\boldsymbol{e}_p]_{\gamma_p}, \boldsymbol{h}'_{c,p}\rangle_{\Gamma_p} + \langle[\boldsymbol{n}\times\boldsymbol{e}_p]_{\gamma_p}, \boldsymbol{h}'_{d,p}\rangle_{\Gamma_p}. \quad (10)$$

The term $\langle[\boldsymbol{n}\times\boldsymbol{e}_p]_{\gamma_p}, \boldsymbol{h}'_{d,p}\rangle_{\Gamma_p}$ is expressed as

$$\langle[\boldsymbol{n}\times\boldsymbol{e}_p]_{\gamma_p}, \boldsymbol{h}'_{d,p}\rangle_{\Gamma_p} = \langle\boldsymbol{n}\times\boldsymbol{e}_p|_{\gamma_p^+}, \boldsymbol{h}'_{d,p}\rangle_{\Gamma_p^+} + \langle\boldsymbol{n}\times\boldsymbol{e}_p|_{\gamma_p^-}, \boldsymbol{h}'_{d,p}\rangle_{\Gamma_p^-}, \quad (11)$$

where the $\boldsymbol{h}'_{d,p}$ is equal to zero on $\Gamma_p^-$ [3]. Therefore, (11) is rewritten

$$\langle[\boldsymbol{n}\times\boldsymbol{e}_p]_{\gamma_p}, \boldsymbol{h}'_p\rangle_{\Gamma_p} = \langle[\boldsymbol{n}\times\boldsymbol{e}_p]_{\gamma_p}, \boldsymbol{h}'_{c,p}\rangle_{\Gamma_p} + \langle\boldsymbol{n}\times\boldsymbol{e}_p|_{\gamma_p^+}, \boldsymbol{h}'_{d,p}\rangle_{\Gamma_p^+}, \quad (12)$$

where the first integral $\langle[\boldsymbol{n}\times\boldsymbol{e}_p]_{\gamma_p},\boldsymbol{h}'_{c,p}\rangle_{\Gamma_p}$ and the second term $\langle\boldsymbol{n}\times\boldsymbol{e}_p|_{\gamma_p^+},\boldsymbol{h}'_{d,p}\rangle_{\Gamma_p^+}$ in the SHS are respectively given in (4) and (5), i.e.

$$\langle[\boldsymbol{n}\times\boldsymbol{e}_p]_{\gamma_p},\boldsymbol{h}'_p\rangle_{\Gamma_p}=\langle\mu_p\beta_p\partial_t(2\boldsymbol{h}_{c,p}+\boldsymbol{h}_{d,p}),\boldsymbol{h}'_p\rangle_{\Gamma_p}+$$

$$\langle\frac{1}{2}\left[\mu_p\beta_p\partial_t(2\boldsymbol{h}_{c,p}+\boldsymbol{h}_{d,p})+\frac{1}{\sigma_p\beta_p}\boldsymbol{h}_{d,p}\right],\boldsymbol{h}'_{d,p}\rangle_{\Gamma_p^+}-\boldsymbol{k}_{f,q}. \quad (13)$$

The $\boldsymbol{k}_{f,q}$ in (13) is a SS defined from the weak form of a previous problem SP $q$, i.e. [6]

$$-\boldsymbol{k}_{f,q}=-\langle\boldsymbol{n}\times\boldsymbol{e}_q|_{\gamma_p^+},\boldsymbol{h}'_{d,p}\rangle_{\Gamma_p^+}=$$

$$\partial_t(\mu_q\boldsymbol{h}_{r,q},\boldsymbol{h}'_q)_{\Omega_q^+=\Gamma_p^+}+\partial_t(\mu_q\boldsymbol{h}_{s,q},\boldsymbol{h}'_q)_{\Omega_q^+=\Gamma_p^+} \quad (14)$$

By combining the equations from (11) to (15), the weak form of the TS model finally becomes

$$\partial_t(\mu_p\boldsymbol{h}_p,\boldsymbol{h}'_p)_{\Omega_p}+\langle\mu_p\beta_p\partial_t(2\boldsymbol{h}_{c,p}+\boldsymbol{h}_{d,p}),\boldsymbol{h}'_p\rangle_{\Gamma_p}+$$

$$+\langle\frac{1}{2}\left[\mu_p\beta_p\partial_t(2\boldsymbol{h}_{c,p}+\boldsymbol{h}_{d,p})+\frac{1}{\sigma_p\beta_p}\boldsymbol{h}_{d,p}\right],\boldsymbol{h}'_{d,p}\rangle_{\Gamma_p^+}$$

$$+\partial_t(\mu_q\boldsymbol{h}_{r,q},\boldsymbol{h}'_q)_{\Omega_q^+=\Gamma_p^+}+\partial_t(\mu_q\boldsymbol{h}_{s,q},\boldsymbol{h}'_q)_{\Omega_q^+=\Gamma_p^+}$$

$$+\langle\boldsymbol{n}\times\boldsymbol{e}_p,\boldsymbol{h}'_p\rangle_{\Gamma_{e,p}-\gamma_p}=0,\forall\,\boldsymbol{h}'_p\in\boldsymbol{H}^1_{h,p}(\mathrm{curl},\Omega_p). \quad (15)$$

At the discrete level, the SSs $\boldsymbol{h}_{r,q}$ and $\boldsymbol{h}_{s,q}$ initially defined the mesh of SP $q$ are transferred to the mesh of the SP $p$ through a projection method [11].

***Step 3: A weak form for volume correction – SP k***

The weak form for the volume correction SP $k$ is presented as

$$\partial_t(\mu_k\boldsymbol{h}_k,\boldsymbol{h}'_k)_{\Omega_p}+(\sigma_k^{-1}\mathrm{curl}\,\boldsymbol{h}_k,\mathrm{curl}\,\boldsymbol{h}'_k)_{\Omega_{c,k}}$$
$$+\partial_t(\boldsymbol{b}_{s,k},\boldsymbol{h}'_k)_{\Omega_{c,k}}+(\boldsymbol{e}_{s,k},\mathrm{curl}\,\boldsymbol{h}'_k)_{\Omega_{c,k}}$$
$$+\langle\boldsymbol{n}\times\boldsymbol{e}_k,\boldsymbol{h}'_k\rangle_{\Gamma_{e,k}-\gamma_k}+\langle[\boldsymbol{n}\times\boldsymbol{e}_k]_{\gamma_k},\boldsymbol{h}'_k\rangle_{\Gamma_k}=0,$$
$$\forall\,\boldsymbol{h}'_k\in\boldsymbol{H}^1_{h,k}(\mathrm{curl},\Omega_k). \quad (16)$$

By substituting VSs $\boldsymbol{b}_{s,k}$ in (6) and $\boldsymbol{e}_{s,k}$ in (7) into (17), one becomes

$$\partial_t(\mu_k\boldsymbol{h}_k,\boldsymbol{h}'_k)_{\Omega_p}+(\sigma_k^{-1}\mathrm{curl}\,\boldsymbol{h}_k,\mathrm{curl}\,\boldsymbol{h}'_k)_{\Omega_{c,k}}$$
$$+\partial_t((\mu_k-\mu_p)(\boldsymbol{h}_q+\boldsymbol{h}_p),\boldsymbol{h}'_k)_{\Omega_{c,k}}$$
$$+(-(\boldsymbol{e}_q+\boldsymbol{e}_p),\mathrm{curl}\,\boldsymbol{h}'_k)_{\Omega_{c,k}}$$
$$+\langle\boldsymbol{n}\times\boldsymbol{e}_k,\boldsymbol{h}'_k\rangle_{\Gamma_{e,k}-\gamma_k}+\langle[\boldsymbol{n}\times\boldsymbol{e}_k]_{\gamma_k},\boldsymbol{h}'_k\rangle_{\Gamma_k}=0,$$
$$\forall\,\boldsymbol{h}'_k\in\boldsymbol{H}^1_{h,k}(\mathrm{curl},\Omega_k). \quad (17)$$

where the fields ($\boldsymbol{h}_q$ in SP $q$ and $\boldsymbol{h}_p$ in SP $p$) are projected from the meshes of the SP $q$ and the SP $p$ to the mesh of SP $k$ through a projection method [11].

In addition, the representation of the TS model ($\langle[\boldsymbol{n}\times\boldsymbol{e}_k]_{\gamma_k},\boldsymbol{h}'_k\rangle_{\Gamma_k}$) in (18) needs to be removed by a SS, i.e. [4-7]

$$\langle[\boldsymbol{n}\times\boldsymbol{e}_k]_{\gamma_k},\boldsymbol{h}'_k\rangle_{\Gamma_k}=-\langle[\boldsymbol{n}\times\boldsymbol{e}_p]_{\gamma_k},\boldsymbol{h}'_k\rangle_{\Gamma_k}. \quad (18)$$

It should be noted that the electric fields $\boldsymbol{e}_q$ and $\boldsymbol{e}_p$ in (17) are unknown and need to be defined via an electric problem presented in next Section.

***Weak formulation for electric problem***

As mentioned in the previous Section, the source quantities $\boldsymbol{e}_q$ and $\boldsymbol{e}_p$ in (17) are found via an electric problem in $\Omega_{c,i}$ ($i$ = $q$, $p$) [9]. The weak form for the electric problem for the volume correction SP $k$ is obtained from the associated (1 c), the unknown electric vector potential $\boldsymbol{u}_k$ ($\boldsymbol{d}_k=\mathrm{curl}\,\boldsymbol{u}_k$) and the constitutive law ($\boldsymbol{d}_k=\epsilon_k\boldsymbol{e}_k$), i.e.

$$(\partial_t(\mu_k\boldsymbol{h}_k),\boldsymbol{u}'_k)_{\Omega_{c,k}}+(\epsilon_k^{-1}\mathrm{curl}\,\boldsymbol{u}_k,\mathrm{curl}\,\boldsymbol{u}'_k)_{\Omega_{c,k}}+$$
$$+\langle\boldsymbol{n}\times\boldsymbol{e}_k,\boldsymbol{u}'_k\rangle_{\Gamma_{c,k}}=0,\forall\,\boldsymbol{u}'_k\in\boldsymbol{H}^1_{h,k}(\mathrm{curl},\Omega_{c,k}), \quad (19)$$

where $\boldsymbol{H}^1_{h,k}(\mathrm{curl},\Omega_{c,k})$ is a function space defined in $\Omega_{c,k}$ including the basis function $\boldsymbol{u}_k$ and test function $\boldsymbol{u}'_k$ as well. The expression for each test function $\boldsymbol{u}'_k$ can be directly written only for non-conducting region $\Omega_{c,k}^C=\Omega_k\backslash\Omega_{c,k}$, i.e. [9]

$$(\epsilon_k^{-1}\mathrm{curl}\,\boldsymbol{u}_k,\mathrm{curl}\,\boldsymbol{u}'_k)_{\Omega_{c,k}}+(\partial_t(\mu_k\boldsymbol{h}_k),\boldsymbol{u}'_k)_{\Omega_{c,k}}+$$
$$(\partial_t(\mu_k\boldsymbol{h}_k),\boldsymbol{u}'_k)_{\Omega_k\backslash\Omega_{c,k}}+(\sigma_k^{-1}\mathrm{curl}\,\boldsymbol{u}_k,\mathrm{curl}\,\boldsymbol{u}'_k)_{\Omega_k\backslash\Omega_{c,k}}$$
$$+\langle\boldsymbol{n}\times\boldsymbol{e}_k,\boldsymbol{u}'_k\rangle_{\partial\Gamma_{c,k}^C}=0,\forall\,\boldsymbol{u}'_k\in\boldsymbol{H}^1_{h,k}(\mathrm{curl},\Omega_{c,k}). \quad (20)$$

In the (20), the source field $\boldsymbol{h}_k$ is transferred from mesh of previous meshes to the mesh of $\Omega_{c,k}$. The volume integrals in $\Omega_k\backslash\Omega_{c,k}$ are defined in a single layer of FEs touching $\partial\Omega_{c,k}$ in $\Omega_k\backslash\Omega_{c,k}$. The solution $\boldsymbol{u}_k$ obtained from (20) is considered as a source for computing the electric field.

## 4. NUMERICAL TESTS

The first application problem is a TEAM workshop problem 28 [13] (Fig. 2). It consists of two stranded inductors and an above shielding plate, for $\mu_{plate}=100,\sigma_{plate}=34$ MS/m, $f=50$ Hz. The inner inductor has $w_1$ = 960 turns and the outer inductor $w_2$ = 576 turns. The sinusoidal currents flow in the inductors in opposite directions, i.e. $i(t)=20\sin(2\pi ft)\,(A)$.

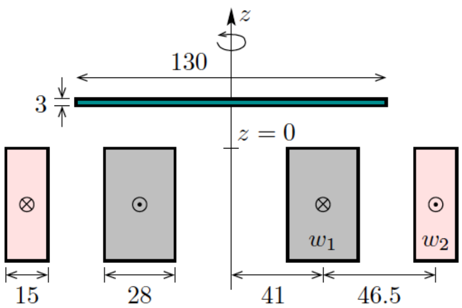


**Fig. 2. Geometry 2-D of TEAM problem 28 (dimensions in mm) [14].**

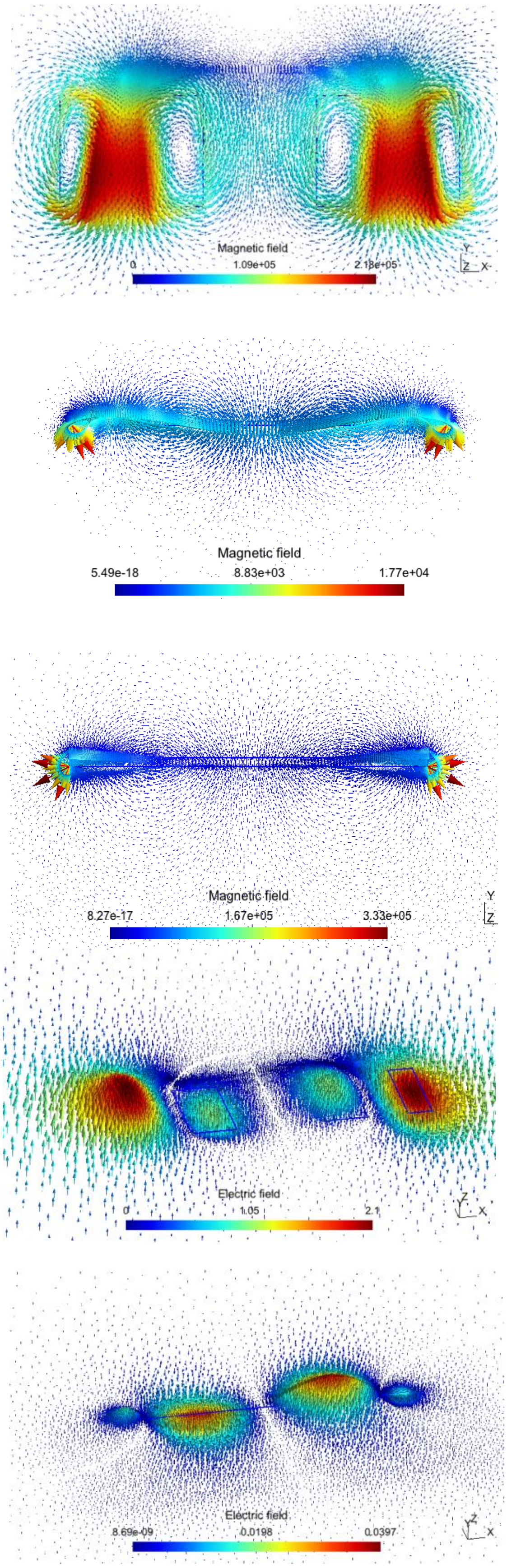


**Fig. 3. Sequence of associated solutions: distribution of magnetic field (real part) for the SP $q$ ($\boldsymbol{h}_q$, *top, inductors alone*), added TS solution SP $p$ ($\boldsymbol{h}_p$, *second level*), electric field for SP $q$ ($\boldsymbol{e}_q$, *third level*), electric field for SP $p$ ($\boldsymbol{e}_p$, *fourth level*) and volume correction SP $k$ ($\boldsymbol{h}_k$, *bottom*).**

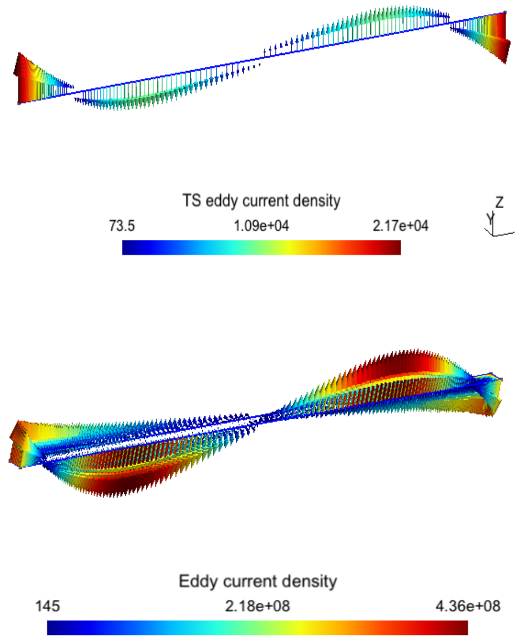


**Fig. 4. Colored map of eddy current density on the TS solution ($\boldsymbol{j}_p$, *top*) and the volume correction ($\boldsymbol{j}_k$, *bottom*) ($\mu_{plate} = 100, \sigma_{plate} = 34$ MS/m, $f = 50$ Hz).**

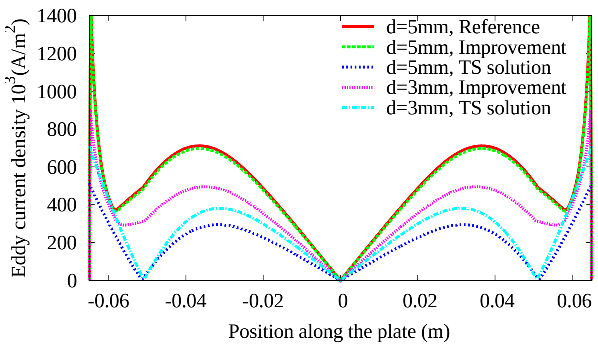


**Fig 5. Eddy current density (*top*) and joule power loss density (*bottom*) of the TS, improvement and reference solutions along the shielding plate for different thicknesses ($\mu_{plate} = 100, \sigma_{plate} = 34$ MS/m, $f = 50$ Hz).**

The test problem is solved with three steps. The sequence of associated solutions on magnetic fields and electric fields of each SPs are shown in Figure 3. A problem with the stranded inductors alone SP $q$ without including a thin shielding is first solved (Fig. 3, *top*, $\boldsymbol{h}_q$). A TS solution SP $p$ with reduced domain that does not contain the inductors any more is then added (Fig. 3, *second level*, $\boldsymbol{h}_p$). The source electric fields $\boldsymbol{e}_q$ and $\boldsymbol{e}_p$ obtained from SP $q$ and SP $p$ are respectively indicated in Fig. 3 (*third level*) and Fig. 3 (*fourth level*). These source fields are projected to the volume correction SP $k$ covering a local thin plate and it surrounding to improve errors on the TS FE solution (Fig. 3, *bottom*, $\boldsymbol{h}_k$).

The colored map of eddy current density on the TS solution and volume correction is pointed in Figure 4. The significant inaccuracy on the eddy current density along the plate of TS SP $p$ corrected by the volume improvement SP $k$ are shown in Figure 6. It reaches 64%, with $\delta$ = 1.22mm and $d$ = 5mm, or lower than 30%

for $d$ = 3 mm. The improvement solution is then compared to be very similar the reference solutions obtained from the classical finite element method [1].

The second application is also based on a TEAM workshop problem 21 (model, B) [14]. The problem is solved in 3-D case and is performed as the same sequence of the previous test. The significant errors on the eddy current are depicted by colored maps with thickness $d$ = 1.5 mm and $d$ = 7.5 mm (from *left* to *right*) (Fig. 6). The relative improvement on the joule power loss along the quarter-plate, from the middle to the end, with the different thicknesses, is presented in Figure 7. It can be up to 60% near the end of the TS for $d$ = 7.5mm, and 40% with $d$ = 1.5mm, for $\mu_{plate} = 100, \sigma_{plate} = 6.484$ MS/m and $f = 50$ Hz in both cases.

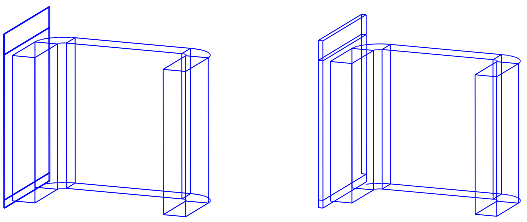

**Fig. 6. Colored map on the eddy current densities showing the regions with the relative volume improvements greater than 5% for d = 1.5 mm and 10 mm (from *left* to *right*), $\mu_{plate} = 100, \sigma_{plate} = 6.484$ MS/m, $f = 50$ Hz).**

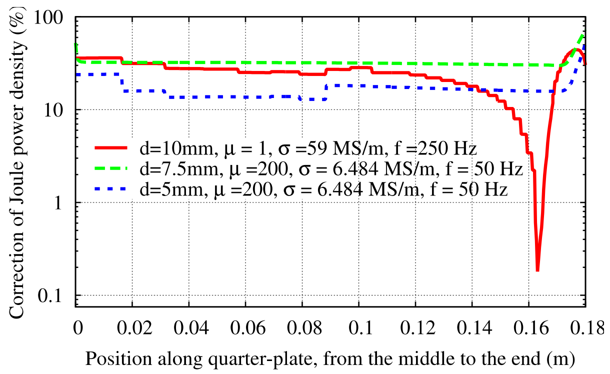


**Fig 7. Relative improvement of joule power loss (3D) along the quarter-plate, from the middle to the end, with different thicknesses ($\mu_p = 200, \sigma_{plate} = 6.484$ MS/m, $f = 50$ Hz).**

## 5. CONCLUSION

The subproblem FE technique has been successfully proposed with $\boldsymbol{h}$-conformal formulation for imporving the errors on the local quantities of the TS model in three steps. The sequence of each step is implemented on its own sub-domain without staring again a full domain. From this step to another one is contrained via VSs and SSs. In particular, an electric problem has been also introduced in the heart of method to strongly support the VSs in volume correction.

The method has been sucessfully applied to the international problems (TEAM workshop problem 21 (model B) and problem 28). The simulated results of the method are checked to be quite similar to the reference solution calculated from the finite element method [1]. This is a very good agreement of the studied method.

The development has been done with the linear case in the frequency domain. It can be extended to the nonlinear case and time domain in the future work.

## NOMENCLATURE

The list of symbols used in the paper is given below:

| | |
|---|---|
| $H^1_{e,q}(\mathrm{curl}, \Omega_q)$ | Curl-conform function space in $\Omega_q$ |
| $(\cdot, \cdot)$ | Volume integral of the product of its vector field argument |
| $< \cdot, \cdot >$ | Surface integral of the product of its vector field argument |
| $\boldsymbol{h_q}$ | Magnetic field (A/m) |
| $\boldsymbol{b_q}$ | Magnetic flux density (T) |
| $\boldsymbol{e_q}$ | Electric field (V/m) |
| $\boldsymbol{d_q}$ | Electric flux density (C/m$^2$) |
| $\boldsymbol{j_{s,q}}$ | Electric current density (A/m$^2$) |
| $\boldsymbol{j_q}$ | Eddy current density (A/m$^2$) |
| $\boldsymbol{b_{s,q}}, \boldsymbol{e_{s,q}}$ | Volume sources |
| $\boldsymbol{k_{f,q}}$ | Surface source field |
| $\boldsymbol{\Omega_q}$ | Bounded open set of E$^3$ |
| $\boldsymbol{\Gamma_q}$ | Boundary of $\Omega_q$ ($\Gamma_q = \partial\Omega_q$) |
| $\boldsymbol{\mu}$ | Magnetic permeability (H/m) |
| $\boldsymbol{\mu_r}$ | Relative magnetic permeability |
| $\boldsymbol{\sigma}$ | Electric conductivity (S/m) |
| $\boldsymbol{\epsilon}$ | Electric permittivity (F/m) |
| $\boldsymbol{\rho}$ | Electric charge (C/ m$^3$) |

## REFERENCES

[1] S. Koruglu, P. Sergeant, R.; Sabarieqo, Vuong; Dang, M.; Wulf. 2011. Influence of contact resistance on shielding efficiency of shielding gutters for high-voltage cables. *IET Electric Power Applications*, vol.5, no.9, pp. 715-720.

[2] L. Krahenbuhl, D. Muller. Thin layers in electrical engineering. Examples of shell models in analyzing eddy- currents by boundary and finite element methods. 1993. *IEEE Trans. Magn*., vol. 29, no. 2, pp. 1450–1455, 1993.

[3] C. Geuzaine, P. Dular, W. Legros. 2000. Dual formulations for the modeling of thin electromagnetic shells using edge elements. *IEEE Trans. Magn*., vol. 36, no. 4, pp. 799–802.

[4] P. Dular, Vuong.; Dang, R.; Sabariego, L. Krahenbuhl and C. Geuzaine. 2011. Correction of Thin Shell Finite Element Magnetic Models via a Subproblem Method. *IEEE Trans. Magn*., vol. 47, no. 5, pp. 1158–1161.

[5] Vuong.; Dang, P. Dular, R. V. Sabariego, L. Krahenbuhl, C. Geuzaine. 2012. Subproblem Approach for Thin Shell Dual Finite Element Formulations. *IEEE Trans. Magn*., vol. 48, no. 2, pp. 407–410.

[6] Vuong.; Dang, P. Dular R.V. Sabariego, L. Krähenbühl, C. Geuzaine. 2013. Subproblem Approach for Modelding Multiply Connected Thin Regions with an h-Conformal Magnetodynamic Finite Element Formulation. *In EPJ AP.*, vol. 63, no.1.

[7] Vuong Dang Quoc, Chistophe Geuzaine. 2019. Using edge elements for mdoeling of 3-D Magnetodynamic Problem via a Subproblem Method. *Sci. Tech. Dev. J.* ; 23(1) :439-445.

[8] P. Dular, R. V. Sabariego, C. Geuzaine, M.; Luz, P.; -Peng, L. Krahenbuhl. 2010. Finite Element Magnetic Models via a Coupling of Subproblems of Lower Dimensions. *IEEE Trans. Magn.*, vol. 46, no. 8, pp. 2827–2830.

[9] P. Dular, R. ; Sabariego. 2007. A perturbation method for computing field distortions due to conductive regions with *h*-conform magnetodynamic finite element formulations. *IEEE Trans. Magn.,* vol. 43, no. 4, pp. 1293-1296.

[10] Dang Quoc Vuong, Nguyen Duc Quang. 2019. Coupling of Local and Global Quantities by A Subproblem Finite Element Method – Application to Thin Region Models. *Adv. Sci. Technol. Eng. Syst. J.* 4(2), 40-44.

[11] Vuong Dang Quoc and Christophe Geuzaine. 2020. Two-way coupling of thin shell finite element magnetic models via an iterative subproblem method. *COMPEL - The international journal for computation and mathematics in electrical and electronic engineering*. ahead-of-print. doi :10.1108/COMPEL-01-2020-0035.

[12] G. Parent, P. Dular, J.; Ducreux, F. Piriou. 2008. Using a galerkin projection method for coupled problems. Magnetics. *Trans. Magn.,* vol 44, no. 6, pp. 830–833.

[13] Hans Karl, Joachim Fetzer, Stefan Kurz, Gunther Lehner, Wolfgang.; Rucker. Description of TEAM Workshop Problem 28: *An Electrodynamic Levitation Device*. https://www.compumag.org

[14] Zhiguang CHENG1, Norio TAKAHASHI, Behzad FORGHANI. 2009. TEAM Problem 21 Family Approved by the International Compumag Society Board at Compumag. *Florianopolis, Brazil*.